THE JOURNAL OF PHYSICAL CHEMISTRY A

Article

pubs.acs.org/JPCA

Mixed Quantum/Classical Theory for Molecule−Molecule Inelastic Scattering: Derivations of Equations and Application to N_2 + H_2 System

Alexander Semenov and Dmitri Babikov*

Chemistry Department, Wehr Chemistry Building, Marquette University, Milwaukee, Wisconsin 53201-1881, United States

ABSTRACT: The mixed quantum classical theory, MQCT, for inelastic scattering of two molecules is developed, in which the internal (rotational, vibrational) motion of both collision partners is treated with quantum mechanics, and the molecule−molecule scattering (translational motion) is described by classical trajectories. The resultant MQCT formalism includes a system of coupled differential equations for quantum probability amplitudes, and the classical equations of motion in the mean-field potential. Numerical tests of this theory are carried out for several most important rotational state-to-state transitions in the N_2 + H_2 system, in a broad range of collision energies. Besides scattering resonances (at low collision energies) excellent agreement with full-quantum results is obtained, including the excitation thresholds, the maxima of cross sections, and even some smaller features, such as slight oscillations of energy dependencies. Most importantly, at higher energies the results of MQCT are nearly identical to the full quantum results, which makes this approach a good alternative to the full-quantum calculations that become computationally expensive at higher collision energies and for heavier collision partners. Extensions of this theory to include vibrational transitions or general asymmetric-top rotor (polyatomic) molecules are relatively straightforward.

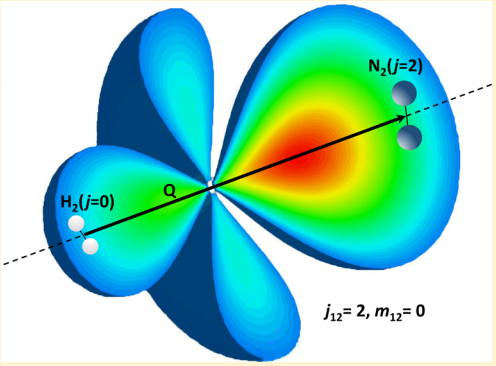

I. INTRODUCTION

Inelastic scattering of two gas-phase molecules is a fundamental physical process important in the atmosphere,[1] combustion,[2] laboratory experiments,[3] and outer space.[4] The simplest version of the process is a rotationally inelastic collision where just the rotational state of one collision partner changes (rotational excitation or quenching), but the processes where the rotational states of both partners change (quasi-resonant energy transfer) are also important.[5] Often, the low-energy vibrational states (bending, torsion) participate in the process too, leading to the coupled ro-vibrational transitions.[6] In the processes where the collision energy is high, so that the vibrational excitation is significant, the collision-induced dissociation of the molecule may occur,[7] which is also an example (the limiting case) of the inelastic scattering.

Theoretical and computational description of these processes is a challenging task. The exact quantum mechanical treatment of rotational transitions usually employs the coupled-channel (CC) formalism developed in 1960s.[8] This approach had great success in simple systems. Thus, CC calculations for collision of a diatomic molecule with an atom are very efficient and computationally affordable, even at higher energies and for heavier molecules and quenchers.[9] However, CC calculations for a triatomic molecule + atom are much more demanding.[10] The diatomic + diatomic[11] and the triatomic + diatomic[5] calculations are computationally challenging, especially for heavy molecules and at higher energies.[12] To make them more affordable, the coupled-states (CS) approximation is often employed,[10] which neglects transitions between different m-states, within the same rotational energy level. Still, the quantum CC calculations for rotational transitions in triatomic + triatomic systems, such as H_2O + H_2O collisions at room temperature, remain computationally unaffordable. Inclusion of vibrational states (in addition to the rotational states) is possible within the CC formalism,[13] but such ro-vibrational calculations are even more demanding.

Thus, the range of applications of the quantum approach remains limited to simple molecules (small number of internal quantum states), light masses, and low collision energies (small number of the partial scattering waves). The classical trajectory method, on the other side, is applied to larger systems at high scattering energies to study the collisional energy transfer.[14] This method is quite affordable computationally, but several flaws of the purely classical approach are also well-known. Among them are zero-point energy leakage,[15] inability to incorporate symmetry restrictions into state-to-state transitions,[16] absence of tunneling,[17] or scattering resonances.[18]

It is an old idea to combine classical mechanics with quantum mechanics in a mixed (or hybrid) approach to the inelastic

Special Issue: Dynamics of Molecular Collisions XXV: Fifty Years of Chemical Reaction Dynamics

Received: July 15, 2015
Revised: August 26, 2015
Published: August 31, 2015

DOI: 10.1021/acs.jpca.5b06812
J. Phys. Chem. A 2015, 119, 12329−12338

scattering to use benefits offered by both classical and quantum frameworks, and trying to avoid the disadvantages of both. It would be attractive to use quantum description of the internal quantized states of the molecules (the vibrational and/or rotational motion), whereas classical mechanics is employed for description of the translational motion of collision partners (the scattering process). In this way, the quantum treatment of continuum motion is avoided, leading to significant computational advantage, but the state-to-state transitions are described rather rigorously, including many quantum effects, such as level quantization, zero-point energy, symmetry of wave functions and associated selection rules, etc.

Some early references on implementations of these ideas date back to the work of McCann and Flannery in 1970s,[19,20] but the most popular and noticeable quantum/classical approach appeared in the 1980s and 1990s due to the work of Billing.[21,22] He introduced two different versions of the quantum/classical theory. His major focus was on the method for description of *ro-vibrational* processes, where quantum mechanics is used for description of the vibrational motion only, whereas classical mechanics is used for both the translational motion of the collision partners and for their rotational motion. When thinking about this approach, we can draw a useful parallel with statistical mechanics. Namely, for statistical description of molecular processes the translational and rotational partition functions are normally computed in the high-temperature limit (equivalent to the classical limit), whereas the vibrational partition function is always a sum over the quantized states. Thus, the mixed quantum/classical approach of Billing is well justified for many molecular systems in a broad range of collision conditions. It was applied to several model systems and several simple real systems[22] and showed great promise. Unfortunately, due to the tragically early death of Billing in 2002,[23] the quantum/classical approach remained not fully developed and this research direction was, basically, abandoned, for a while.

The opportunity of using a mixture of quantum and classical mechanics was called to memory only recently,[24−26] for the studies of ozone formation reaction O + O_2 + Ar, which is a recombination reaction that includes formation and stabilization of highly excited ro-vibrational states of O_3, or scattering resonances, a very complex process for which no standard approach or well-developed method exist. This interesting application stimulated a new round of theory developments,[27,28] including the second version of quantum/classical theory, with emphasis on *quantum treatment of rotation.*[29] In his early work, Billing also developed a method where the rotation of a diatomic molecule (treated as rigid rotor, no vibration) was described quantum mechanically, whereas the scattering of an atom off the diatomic was treated classically.[30] Surprisingly, one can find very limited applications of this method in the literature. Billing himself applied it to just one simple system, He + H_2, at just two scattering energies, looking at transitions between the lowest energy levels only.[22,30] Although his results were encouraging, more detailed studies have never been pursued, to the best of our knowledge. One reason for this could be that at that time the full-quantum scattering calculations (to compare with) were also quite limited. In any case, this second mixed quantum/classical method, focused on the quantum treatment of rotation, was abandoned as well.

The mixed quantum classical theory (MQCT) we developed recently is similar to this second method of Billing in many respects. We also describe the rotational motion quantum mechanically, by expanding the rotational wave function over the basis set of rotational eigenstates with time-dependent expansion coefficients, and we also describe scattering of collision partners using classical trajectories, driven by the mean-field potential. However, we went much further in theory development, testing, and applications. First of all, we worked out the MQCT formalism in both the space-fixed (SF) reference frame and the body-fixed (BF) reference frame[29] and carried out calculations on a model system to demonstrate that both versions are physically equivalent and both theories, equations, and computer codes are correct. We quickly learned that the SF version of MQCT is numerically inefficient,[31] because the corresponding state-to-state transition matrix (which governs evolution of the rotational wave function) is complex-valued with dense structure and each matrix element dependent on three classical variables (that evolve along the collision trajectory). Luckily, we found that the BF version of MQCT, in contrast, involves a real-valued sparse state-to-state transition matrix with simple bock-diagonal structure, and each element is dependent on the molecule-quencher separation only—just one classical variable.[29] In the work that followed[32−35] we demonstrated that this BF version of MQCT is numerically efficient.

For example, for the fully coupled MQCT the scaling law, which is computational cost vs number of channels, is $n^{2.5}$, and this is only slightly better than n^3 scaling of the full-quantum CC calculations.[34,35] Note, however, that here n is the number of included rotational energy levels at one representative collision energy, and it should not be forgotten that the cost of converging the full-quantum calculations with respect to the number of *partial waves* also increases when the collision energy is raised, leading in practice to the total cost in the range of n^5 to n^6. In contrast, MQCT has no such "overhead", because scattering of the quencher is treated classically. Thus, the scaling properties of MQCT are superior, and the advantages are particularly significant for heavier collision partners and at higher collision energies. Interestingly, within MQCT one can also formulate the CS approximation,[33] which gives another source of speed-up, by a factor of roughly ×20.[35] It is worth noting that Billing used only such CS version of his quantum classical theory, whereas our focus is on the fully coupled MQCT approach, which appears to be surprisingly accurate when compared to the full-quantum CC method.

To access the accuracy of MQCT, we conducted very detailed and hierarchical benchmark studies for several real molecule + atom systems. We applied it to heavy and light collision partners, at low and high scattering energies in a broad range, to study rotational excitation and quenching, of the low-lying and highly excited rotational states, computing total and differential, elastic and inelastic cross sections, and we even looked at the simplest ro-vibrational transitions. We started with diatomic + atom systems and studied N_2 + Na[32,33] and H_2 + He.[33] Then we moved to the symmetric top rotors, such as CH_3 radical and NH_3 collided with He (unpublished) and, finally, extended MQCT to treat the general case of an asymmetric top rotor + atom. This was applied to H_2O + He[34] and, most impressively, to $HCOOCH_3$ + He,[35] which is the largest molecule (methyl formate) ever considered for the inelastic scattering calculations. In all these systems we saw that at higher collision energies MQCT gives results nearly identical to the full-quantum results and remains computationally cheap (e.g., up to collision energies of 10 000 cm^{-1} in the case of H_2O + He).[34] At low collision energies the excitation thresholds are predicted correctly (e.g., in N_2 + Na)[32,33] and, the results of MQCT remain reasonably

DOI: 10.1021/acs.jpca.5b06812
J. Phys. Chem. A 2015, 119, 12329−12338

accurate down to collision energies of just few wavenumbers. We also learned how to use *phase information* to reproduce quantum interference and construct the differential over scattering angle cross sections (e.g., in N_2 + Na)[32,33] but still have to find a way to describe scattering resonances. This seems to be feasible,[36] but at present we simply remove the orbiting trajectories, and focus on nonresonant contribution to cross sections (e.g., in $HCOOCH_3$ + He).[35] Importantly, we never saw MQCT failing miserably.

This paper is focused on another important development of MQCT: its extension onto the molecule + molecule systems, the case that is particularly demanding to treat computationally using the full-quantum approach. There are many important molecule + molecule systems that could be studied using MQCT, including small organic molecules and linear carbon chains relevant to astrophysical environments collided with H_2,[4] small polyatomic molecules in the atmosphere collided with O_2 and N_2, and triatomic molecules collided with H_2O, including water−water collisions.

The paper is organized as follows. In section II we outline the theory for MQCT calculations of scattering of two diatomic molecules. In section III we present numerical results for N_2 + H_2 system. Conclusions are given and future research directions are discussed in section IV.

II. THEORY

II.1. Quantum and Classical Degrees of Freedom. Consider collisions of two molecules: Molecule 1 is AB and molecule 2 is CD, as shown in Figure 1. Classical variables that

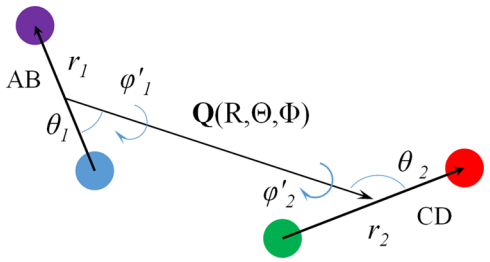

Figure 1. Classical and quantum variables for description of inelastic collision of two diatomic molecules in the body-fixed reference frame.

describe molecule−molecule scattering are three coordinates (R, Θ, Φ) of the vector **Q** that connects the centers of mass of two molecules. Quantum degrees of freedom are four angles (θ_1, θ_2, φ'_1, φ'_2) needed to describe positions of two diatomics with respect to vector **Q** (i.e., in the BF reference frame). As in the earlier paper[29] we use *primed* variables and indexes for the BF reference frame (e.g., φ', m'), to distinguish from those in the SF reference frame. The interatomic distances r_1 and r_2 are considered to be fixed for simplicity (rigid rotors), but they can be easily introduced into the formalism for description of ro-vibrational processes, just as it was done in our earlier work on the molecule−atom systems.[29]

Rotation of each molecule is quantized and is described by the corresponding rotational eigenfunction, $Y_{j_1}^{m_1'}(\theta_1,\varphi_1')$ and $Y_{j_2}^{m_2'}(\theta_2,\varphi_2')$ for molecules 1 and 2, respectively (spherical harmonics in the BF). The total angular momentum of two molecules $\mathbf{j}_{12} = \mathbf{j}_1 + \mathbf{j}_2$ is also quantized. The corresponding eigenfunctions can be expressed through spherical harmonics as follows:[37]

$$\Upsilon_{j_{12}j_1j_2}^{m_{12}'}(\theta_1,\theta_2,\varphi_1',\varphi_2') = \sum_{m_1'm_2'} \langle j_1 m_1' j_2 m_2' | j_{12} m_{12}' \rangle Y_{j_1}^{m_1'}(\theta_1,\varphi_1')\, Y_{j_2}^{m_2'}(\theta_2,\varphi_2') \tag{1}$$

The total time-dependent wave function for the quantum part of the system can be expressed as

$$\psi(\theta_1,\theta_2,\varphi_1',\varphi_2',t) = \sum_{j_{12}m_{12}'j_1j_2} a_{j_{12}j_1j_2}^{m_{12}'}(t)\, \Upsilon_{j_{12}j_1j_2}^{m_{12}'}(\theta_1,\theta_2,\varphi_1',\varphi_2') \exp\{-iE_{j_1j_2}t\} \tag{2}$$

where $a_{j_{12}j_1j_2}^{m_{12}'}$ are time-dependent expansion coefficients, and atomic units are used for energy. The range of values of j_1 and j_2 in this sum defines the basis set size for description of two quantized rotors (e.g., $0 \le j_1 \le j_1^{\max}$ and $0 \le j_2 \le j_2^{\max}$). It depends on physical properties of the system and is a convergence parameter. The value of j_{12} varies in the range $|j_1 - j_2| \le j_{12} \le j_1 + j_2$. The value of m_{12}' varies in the range $-j_{12} \le m_{12}' \le j_{12}$.

To avoid confusion, we want to emphasize that $\mathbf{j}_{12}$ is *not* the orbital angular momentum of the motion of one molecule with respect to the other. The orbital motion (scattering) is described classically in this formalism and is not quantized. It should also be stressed that the four-dimensional functions $\Upsilon_{j_{12}j_1j_2}^{m_{12}'}(\theta_1,\theta_2,\varphi_1',\varphi_2')$ play an accessory role only and do not enter into any final equations of motion (derived below). But, if needed, they can be obtained from eq 1 using spherical harmonics and Clebsch−Gordan coefficients and visualized as we have done in the TOC graphic, which represents the component $j_{12} = 2$, $m_{12} = 0$ for the collision of AB($j_1 = 2$) with CD($j_2 = 0$).

II.2. BF Transformation of Wave Functions. The key point of the BF formulation of MQCT is to describe how the function (2) evolves due to rotation of the intermolecular axis, described by **Q**, in the course of molecule−molecule scattering. For this, we express rotational eigenstates of the molecules 1 and 2 in the BF frame through the rotational eigenstates in the SF frame using Wigner **D**-matrices (see eq 17 in ref 29):

$$Y_{j_1}^{m_1'}(\theta_1,\varphi_1') = \sum_{m_1} D_{m_1m_1'}^{j_1}(\Phi,\Theta,0)\, Y_{j_1}^{m_1}(\theta_1,\varphi_1) \tag{3a}$$

$$Y_{j_2}^{m_2'}(\theta_2,\varphi_2') = \sum_{m_2} D_{m_2m_2'}^{j_2}(\Phi,\Theta,0)\, Y_{j_2}^{m_2}(\theta_2,\varphi_2) \tag{3b}$$

Here, as in the earlier paper,[29] we use *unprimed* variables and indexes for the SF reference frame (e.g., θ, m). Substitution of eqs 3a and 3b into eq 1 gives

$$\Upsilon_{j_{12}j_1j_2}^{m_{12}'}(\theta_1,\theta_2,\varphi_1',\varphi_2') = \sum_{m_1'm_2',m_1m_2} \langle j_1 m_1' j_2 m_2' | j_{12} m_{12}' \rangle D_{m_1m_1'}^{j_1}(\Phi,\Theta,0) \times D_{m_2m_2'}^{j_2}(\Phi,\Theta,0)\, Y_{j_1}^{m_1}(\theta_1,\varphi_1)\, Y_{j_2}^{m_2}(\theta_2,\varphi_2) \tag{4}$$

The product of two Wigner D-functions in this formula can be simplified as follows (see eq 4.4.1 in ref 38):

$$D_{m_1m_1'}^{j_1}(\Phi,\Theta,0)\, D_{m_2m_2'}^{j_2}(\Phi,\Theta,0) = \sum_{j=|j_2-j_1|}^{j_2+j_1} \sum_{m=-j}^{j} \sum_{k=-j}^{j} \langle j_1 m_1' j_2 m_2' | jm \rangle \langle j_1 m_1 j_2 m_2 | jk \rangle D_{km}^{j}(\Phi,\Theta,0) \tag{5}$$

DOI: 10.1021/acs.jpca.5b06812
J. Phys. Chem. A 2015, 119, 12329−12338

Substitution of eq 5 into eq 4 gives

$$\Upsilon^{m'_{12}}_{j_{12}j_1j_2}(\theta_1,\theta_2,\varphi_1',\varphi_2') = \sum_{m_1'm_2',m_1m_2} \langle j_1 m_1' j_2 m_2' | j_{12} m_{12}' \rangle \times \sum_{j=|j_2-j_1|}^{j_2+j_1} \sum_{m=-j}^{j} \sum_{k=-j}^{j} \langle j_1 m_1' j_2 m_2' | jm \rangle \langle j_1 m_1 j_2 m_2 | jk \rangle \times D^j_{km}(\Phi,\Theta,0)\, Y^{m_1}_{j_1}(\theta_1,\varphi_1)\, Y^{m_2}_{j_2}(\theta_2,\varphi_2) \quad (6)$$

Note that in the SF reference frame one could write an expression analogous to eq 1, written for the BF reference frame, namely

$$\Upsilon^{k}_{jj_1j_2}(\theta_1,\theta_2,\varphi_1,\varphi_2) = \sum_{m_1m_2} \langle j_1 m_1 j_2 m_2 | jk \rangle Y^{m_1}_{j_1}(\theta_1,\varphi_1)\, Y^{m_2}_{j_2}(\theta_2,\varphi_2) \quad (7)$$

Comparing eqs 6 and 7, we can establish transformation of the total wave functions Υ between the BF and SF reference frames:

$$\begin{aligned}\Upsilon^{m'_{12}}_{j_{12}j_1j_2}(\theta_1,\theta_2,\varphi_1',\varphi_2') &= \sum_{m_1'm_2'} \langle j_1 m_1' j_2 m_2' | j_{12} m_{12}' \rangle \times \sum_{j=|j_2-j_1|}^{j_2+j_1} \sum_{m=-j}^{j} \sum_{k=-j}^{j} \langle j_1 m_1' j_2 m_2' | jm \rangle D^j_{km}(\Phi,\Theta,0)\, \Upsilon^{k}_{jj_1j_2}(\theta_1,\theta_2,\varphi_1,\varphi_2) \\ &= \sum_{j=|j_2-j_1|}^{j_2+j_1} \sum_{m=-j}^{j} \sum_{k=-j}^{j} D^j_{km}(\Phi,\Theta,0)\, \Upsilon^{k}_{jj_1j_2}(\theta_1,\theta_2,\varphi_1,\varphi_2) \times \sum_{m_1'm_2'} \langle j_1 m_1' j_2 m_2' | j_{12} m_{12}' \rangle \langle j_1 m_1' j_2 m_2' | jm \rangle \end{aligned} \quad (8)$$

The last term of this expression can be simplified using the closure relation:

$$\sum_{m_1'm_2'} \langle j_1 m_1' j_2 m_2' | j_{12} m_{12}' \rangle \langle j_1 m_1' j_2 m_2' | jm \rangle = \langle j_{12} m_{12}' | jm \rangle$$

which converts eq 8 into the following form:

$$\begin{aligned}\Upsilon^{m'_{12}}_{j_{12}j_1j_2}(\theta_1,\theta_2,\varphi_1',\varphi_2') &= \sum_{j=|j_2-j_1|}^{j_2+j_1} \sum_{m=-j}^{j} \sum_{k=-j}^{j} D^j_{km}(\Phi,\Theta,0)\, \Upsilon^{k}_{jj_1j_2}(\theta_1,\theta_2,\varphi_1,\varphi_2) \langle j_{12} m_{12}' | jm \rangle \\ &= \sum_{j=|j_2-j_1|}^{j_2+j_1} \sum_{m=-j}^{j} \sum_{k=-j}^{j} D^j_{km}(\Phi,\Theta,0)\, \Upsilon^{k}_{jj_1j_2}(\theta_1,\theta_2,\varphi_1,\varphi_2) \delta^{j_{12}}_{j} \delta^{m'_{12}}_{k} \\ &= \sum_{k=-j_{12}}^{j_{12}} D^{j_{12}}_{km'_{12}}(\Phi,\Theta,0)\, \Upsilon^{k}_{j_{12}j_1j_2}(\theta_1,\theta_2,\varphi_1,\varphi_2) \end{aligned} \quad (8')$$

To simplify the notation, we can leave out the range of the index k, which gives the following final formula:

$$\Upsilon^{m'_{12}}_{j_{12}j_1j_2}(\theta_1,\theta_2,\varphi_1',\varphi_2') = \sum_{k} D^{j_{12}}_{km'_{12}}(\Phi,\Theta,0)\, \Upsilon^{k}_{j_{12}j_1j_2}(\theta_1,\theta_2,\varphi_1,\varphi_2) \quad (8'')$$

Notice that, qualitatively, this expression is similar to eqs 3a and 3b, which is understood: transformation of rotational wave function in space due to its rotation should not depend on how this wave function is constructed; it should transform just as the corresponding angular momentum, which gives the physical meaning of eq 8″.

II.3. Equations of Motion. Equations of motion for time evolution of the expansion coefficients $a^{m'_{12}}_{j_{12}j_1j_2}$ are obtained by substituting eq 2, with $\Upsilon^{m'_{12}}_{j_{12}j_1j_2}$ expressed by eq 8″, into the time-dependent Schrödinger equation. Derivations are very similar to those in the molecule + atom case, outlined in eqs 18−21 of our earlier paper, ref 29. For the sake of brevity we will not repeat them here and will only present the result

$$\frac{\partial a^{m'_{12}}_{j_{12}j_1j_2}}{\partial t} = -\mathrm{i} \sum_{j'_{12}m''_{12}j'_1j'_2} a^{m''_{12}}_{j'_{12}j'_1j'_2} M^{j_{12}m'_{12}j_1j_2}_{j'_{12}m''_{12}j'_1j'_2}(R) \exp\{\mathrm{i}(E_{j_1j_2} - E_{j'_1j'_2})t\} - \sum_{m''_{12}} a^{m''_{12}}_{j_{12}j_1j_2} W^{m'_{12}}_{m''_{12}} \quad (9)$$

We see that besides phase factors, time evolution of the expansion coefficients is driven by two transition matrices. Matrix $W^{m'_{12}}_{m''_{12}}$ is responsible for transitions between different (energetically degenerate) projection states of the total angular momentum j_{12}. It can be expressed as

$$W^{m'_{12}}_{m''_{12}} = U^{m'_{12}}_{m''_{12}}\dot{\Theta} + \mathrm{i}(\sin\Theta V^{m'_{12}}_{m''_{12}} - m''_{12}\cos\Theta\delta_{m'_{12},m''_{12}})\dot{\Phi} \quad (10)$$

where for convenience we introduced two time-independent matrices:

$$U^{m'_{12}}_{m''_{12}} = \frac{1}{2}\left[\sqrt{j_{12}(j_{12}+1) - m''_{12}(m''_{12}-1)}\,\delta_{m'_{12},m''_{12}-1} - \sqrt{j_{12}(j_{12}+1) - m''_{12}(m''_{12}+1)}\,\delta_{m'_{12},m''_{12}+1}\right] \quad (11a)$$

$$V^{m'_{12}}_{m''_{12}} = \frac{1}{2}\left[\sqrt{j_{12}(j_{12}+1) - m''_{12}(m''_{12}-1)}\,\delta_{m'_{12},m''_{12}-1} + \sqrt{j_{12}(j_{12}+1) - m''_{12}(m''_{12}+1)}\,\delta_{m'_{12},m''_{12}+1}\right] \quad (11b)$$

Matrices $U^{m'_{12}}_{m''_{12}}$ and $V^{m'_{12}}_{m''_{12}}$ have to be computed only once, for every value of j_{12}, but they do not depend on j_1 or j_2. They arecomputed analytically and do not include the interaction potential. Physical meaning of the last term in eq 9 is the centrifugal coupling effect. Allowed transitions are $\Delta m'_{12} = \pm 1$. Neglecting this term leads to CS approximation within MQCT framework, with no transitions allowed between the m'_{12} states. Here we do not follow this path and focus on the fully coupled MQCT. However, eq 10 can be simplified in the case when the initial state of the system is an eigenstate (rather than a wave packet) and the interaction potential is cylindrically symmetric. In this case the trajectory of relative molecule−molecule scattering stays in one plane, which can be chosen as the equatorial plane, $\Theta = \pi/2$, without loss of generality. With this choice, as collision progresses, the classical vector $\mathbf{Q}$ rotates in the equatorial plane, which is described by time evolution of classical variables $R(t)$ and $\Phi(t)$, as one can see in Figure 1. Because $\sin\Theta = 1$, $\cos\Theta = 0$, and $\dot{\Theta} = 0$, eq 10 simplifies significantly, giving

$$W^{m'_{12}}_{m''_{12}} = \mathrm{i}V^{m'_{12}}_{m''_{12}}\dot{\Phi} \quad (12)$$

This formula shows clearly that although $V^{m'_{12}}_{m''_{12}}$ is time-independent, the entire matrix $W^{m'_{12}}_{m''_{12}}$ evolves in time, according to the angular speed $\dot{\Phi}$ of the vector $\mathbf{Q}$ (see below).

DOI: 10.1021/acs.jpca.5b06812
J. Phys. Chem. A 2015, 119, 12329−12338

The second matrix in eq 9 is the potential coupling matrix $M^{j_{12}m'_{12}j_1j_2}_{j'_{12}m''_{12}j'_1j'_2}$ that should be computed numerically, using the potential energy surface $V(R,\gamma_1,\gamma_2,\varphi'_1,\varphi'_2)$, as

$$M^{j_{12}m'_{12}j_1j_2}_{j'_{12}m''_{12}j'_1j'_2}(R) = \langle \Upsilon^{m''_{12}}_{j'_{12}j'_1j'_2}(\gamma_1,\gamma_2,\varphi'_1,\varphi'_2)|V(R,\gamma_1,\gamma_2,\varphi'_1,\varphi'_2)|\Upsilon^{m'_{12}}_{j_{12}j_1j_2}(\gamma_1,\gamma_2,\varphi'_1,\varphi'_2)\rangle \quad (13)$$

Notice that each matrix element is a function of molecule−molecule separation R, which is the length of the vector $\mathbf{Q}$, that itself evolves during the collision (see below). In practice, a useful expression for matrix elements is obtained by expanding the interaction potential over basis set of spherical harmonics:[39]

$$V(R,\theta_1,\theta_2,\varphi'_1,\varphi'_2) = \sum_{l_1l_2} \sqrt{\frac{2l+1}{4\pi}} A_{l_1l_2}(R) \sum_m \langle l_1 m l_2 - m|l0\rangle Y^m_{l_1}(\theta_1,\varphi'_1)\, Y^{-m}_{l_2}(\theta_2,\varphi'_2) \quad (14)$$

This is a formal mathematical expansion of the (real-valued) potential energy function. Here, for two chosen values of l_1 and l_2 the value of l varies in the range $|l_1 - l_2| \le l \le l_1 + l_2$. The basis set size depends on physical properties of the system and is a convergence parameter (e.g., $0 \le l_1 \le l_1^{\max}$ and $0 \le l_2 \le l_2^{\max}$). The value of m varies in the range $\min(l_1,l_2) \le m \le \min(l_1,l_2)$. However, with eq 1, the sum over m in this expression can be eliminated. Substitution of the result into eq 13 gives

$$M^{j_{12}m'_{12}j_1j_2}_{j'_{12}m''_{12}j'_1j'_2}(R) = \sum_{l_1l_2} \sqrt{\frac{2l+1}{4\pi}} A_{l_1l_2}(R) \times \langle \Upsilon^{m'_{12}}_{j_{12}j_1j_2}(\theta_1,\theta_2,\varphi'_1,\varphi'_2)|\Upsilon^0_{l_1l_2}(\theta_1,\theta_2,\varphi'_1,\varphi'_2)|\Upsilon^{m''_{12}}_{j'_{12}j'_1j'_2}(\theta_1,\theta_2,\varphi'_1,\varphi'_2)\rangle \quad (15)$$

In fact, even from here one may see that matrix elements are nonzero only if $m'_{12} = m''_{12}$. This property can be derived in more rigorous way, by using eq 1 in eq 15 three times (for each of the four-dimensional functions Υ), and splitting the four-dimensional integral onto two two-dimensional integrals, as follows:

$$M^{j_{12}m'_{12}j_1j_2}_{j'_{12}m''_{12}j'_1j'_2}(R) = \sum_{l_1l_2} \sqrt{\frac{2l+1}{4\pi}} A_{l_1l_2}(R) \times \sum_{m_1m'_2m''_1m''_2m} \langle l_1 m l_2 - m|l0\rangle \langle j_1 m'_1 j_2 m'_2|j_{12}m'_{12}\rangle \langle j'_1 m''_1 j'_2 m''_2|j'_{12}m''_{12}\rangle \times \langle Y^{m_1}_{j_1}(\theta_1,\varphi'_1)|Y^m_{l_1}(\theta_1,\varphi'_1)|Y^{m''_1}_{j'_1}(\theta_1,\varphi'_1)\rangle \langle Y^{m'_2}_{j_2}(\theta_2,\varphi'_2)|Y^{-m}_{l_2}(\theta_2,\varphi'_2)|Y^{m''_2}_{j'_2}(\theta_2,\varphi'_2)\rangle \quad (16)$$

This formula allows seeing that matrix elements are nonzero not only if $m'_1 = m''_1 + m$ and $m'_2 = m''_2 - m$ (from the integrals) but also only if $m'_{12} = m'_1 + m'_2$ and $m''_{12} = m''_1 + m''_2$ (from the Clebsch−Gordan coefficients). All these conditions can be satisfied simultaneously only if $m'_{12} = m''_{12}$. So, the matrix $\mathbf{M}$ is block-diagonal in m'_{12}, with each block describing transitions from $j_{12}j_1j_2$ to $j'_{12}j'_1j'_2$, within the same value of m'_{12}. For convenience, the index m'_{12} can be omitted from the list of indexes for this matrix, namely, we can write $M^{j_{12}j_1j_2}_{j'_{12}j'_1j'_2}$, meaning that such blocks should be computed for all values of m'_{12}.

Finally, using the two simplifications discussed above, we can rewrite eq 9 in the following convenient form, where transitions between the levels $j_{12}j_1j_2$ (within m'_{12}) are driven by matrix $\mathbf{M}$, whereas transitions between the states m'_{12} (within j_{12}) are driven by matrix $\mathbf{V}$:

$$\frac{\partial a^{m'_{12}}_{j_{12}j_1j_2}}{\partial t} = -\mathrm{i} \sum_{j'_{12}j'_1j'_2} a^{m'_{12}}_{j'_{12}j'_1j'_2} M^{j_{12}j_1j_2}_{j'_{12}j'_1j'_2}(R) \exp\{\mathrm{i}(E_{j_1j_2} - E_{j'_1j'_2})t\} - \mathrm{i} \sum_{m''_{12}} a^{m''_{12}}_{j_{12}j_1j_2} V^{m'_{12}}_{m''_{12}} \dot{\Phi} \quad (17)$$

This is a system of coupled differential equations, of a form quite typical to quantum mechanics (except, maybe, the presence of time-dependent classical variables R and Φ), which can propagated in time using any suitable method, such as general fourth-order Runge−Kutta, or more specialized numerical methods.

The equations of motion for classical degrees of freedom, coordinates $R(t)$ and $\Phi(t)$ of the vector $\mathbf{Q}$, are derived using the Ehrenfest theorem as explained in our earlier work.[29] Interestingly, for the molecule + molecule system studied here, the classical equations come out identical to those we derived earlier for the molecule + atom system.[29,31] This makes sense, simply because the variables R and Φ are exactly the same. Thus, we will not repeat the derivations here, and will only summarize the final equations, for the sake of completeness:

$$\dot{R} = \frac{P_R}{\mu} \quad (18)$$

$$\dot{\Phi} = \frac{P_\Phi}{\mu R^2} \quad (19)$$

$$\dot{P}_R = -\sum_{j'_{12}m''_{12}j'_1j'_2} \sum_{j_{12}m'_{12}j_1j_2} (a^{m''_{12}}_{j'_{12}j'_1j'_2})^* a^{m'_{12}}_{j_{12}j_1j_2} \times \exp\{\mathrm{i}(E_{j'_1j'_2} - E_{j_1j_2})t\} \frac{\partial M^{j'_{12}j'_1j'_2}_{j_{12}j_1j_2}(R)}{\partial R} + \frac{P_\Phi^2}{\mu R^3} \quad (20)$$

$$\dot{P}_\Phi = -\mathrm{i} \sum_{j'_{12}m''_{12}j'_1j'_2} \sum_{j_{12}m'_{12}j_1j_2} (a^{m''_{12}}_{j'_{12}j'_1j'_2})^* a^{m'_{12}}_{j_{12}j_1j_2} \times \exp\{\mathrm{i}(E_{j'_1j'_2} - E_{j_1j_2})t\} [\mathbf{M}, \mathbf{V}]^{j'_{12}m''_{12}j'_1j'_2}_{j_{12}m'_{12}j_1j_2} \quad (21)$$

Here μ is a molecule−molecule reduced mass. Equation 21 includes a commutator of matrices $M^{j'_{12}j'_1j'_2m''_{12}}_{j_{12}j_1j_2}$. These equations can be propagated in time and space numerically, together with equations for quantum degrees of freedom, eq 17. In practice, we compute matrix elements on a predefined grid of points R_i along the coordinate R, just as in the full-quantum approach. During the propagation, when the MQCT trajectory comes to the vicinity of a grid point, we simply spline those precomputed matrix elements using 1D-spline of several points closest to this point. Such a procedure is very efficient and accurate using quadratic or qubic spline, carries little overhead, and is similar to splining the PES (defined on a grid) during propagation of purely classical trajectories.

II.4. Sampling of the Initial Conditions. Our procedure for computing state-to-state cross sections not only includes sampling of the initial conditions for classical degrees of freedom but also incorporates a sum over the final and an average over the initial degenerate states, just as in the full-quantum calculations. Namely, for a state-to-state transition of interest $j_1^{\mathrm{ini}}j_2^{\mathrm{ini}} \to j_1^{\mathrm{fin}}j_2^{\mathrm{fin}}$ a set of $(2j_1^{\mathrm{ini}} + 1)(2j_2^{\mathrm{ini}} + 1)$ independent calculations has to be

DOI: 10.1021/acs.jpca.5b06812
J. Phys. Chem. A 2015, 119, 12329−12338

carried out, with all possible values of the initial j_{12}^{ini} and $m_{12}'^{ini}$ needed to construct the average:

$$\sigma_{j_1^{ini} j_2^{ini} \to j_1^{fin} j_2^{fin}} = \frac{1}{(2j_1^{ini}+1)(2j_2^{ini}+1)} \times \sum_{j_{12}^{ini}=|j_1^{ini}-j_2^{ini}|}^{j_1^{ini}+j_2^{ini}} \left(\sum_{m_{12}'^{ini}=-j_{12}^{ini}}^{j_{12}^{ini}} \sigma_{j_{12}^{ini} m_{12}'^{ini} j_1^{ini} j_2^{ini} \to j_1^{fin} j_2^{fin}} \right) \quad (22)$$

For each of these calculations we sample randomly and uniformly the value of J that corresponds to the total angular momentum in the problem, through the range $0 \le J \le J^{max}$. The value of J^{max} is a convergence parameter, just as in the full-quantum calculations. For a given pair of j_{12}^{ini} and J we sample the value of l randomly and uniformly through the range $|J - j_{12}^{ini}| \le l \le J + j_{12}^{ini}$. It corresponds to the orbital angular momentum in the molecule−molecule system, $\mathbf{l} = \mathbf{J} - \mathbf{j}_{12}$, and is used to define classical initial conditions as follows:

$$P_\Phi = \sqrt{l(l+1)} \quad (23)$$

$$P_R = \sqrt{2\mu E - {P_\Phi}^2/R^2} \quad (24)$$

where E is the kinetic energy of collision (not the total energy) and R is the initial molecule−molecule separation (about 25 Bohr). The initial value of Φ is arbitrary, and we use $\Phi = 0$. Note that although l is closely related to the classical collision impact parameter, we do not sample or use the impact parameter directly. The goal is keep MQCT as close as possible to the quantum formalism.

With the initial conditions of eqs 23 and 24, the classical-like eqs 18−21 and a system of quantum-like coupled eqs 17 are propagated through the collision event, until the point when the molecule−molecule separation exceeds the initial limiting value. The final values of probability amplitudes are used to compute transition probability (summed over the degenerate final states):

$$P^{(i)}_{j_{12}^{ini} m_{12}'^{ini} j_1^{ini} j_2^{ini} \to j_1^{fin} j_2^{fin}} = \sum_{j_{12}^{fin}=|j_1^{fin}-j_2^{fin}|}^{j_1^{fin}+j_2^{fin}} \sum_{m_{12}'^{fin}=-j_{12}^{fin}}^{j_{12}^{fin}} P^{(i)}_{j_{12}^{ini} m_{12}'^{ini} j_1^{ini} j_2^{ini} \to j_{12}^{fin} m_{12}'^{fin} j_1^{fin} j_2^{fin}} = \sum_{j_{12}^{fin}=|j_1^{fin}-j_2^{fin}|}^{j_1^{fin}+j_2^{fin}} \sum_{m_{12}'^{fin}=-j_{12}^{fin}}^{j_{12}^{fin}} |a^{m_{12}'^{fin}}_{j_{12}^{fin} j_1^{fin} j_2^{fin}}|^2 \quad (25)$$

Here index i labels independent trajectories in a batch of N trajectories. This number is also a convergence parameter (here, around 200 per one initial state, per energy point). Average of probability over the batch gives the cross section:

$$\sigma_{j_{12}^{ini} m_{12}'^{ini} j_1^{ini} j_2^{ini} \to j_1^{fin} j_2^{fin}} = \frac{\pi J_{max}}{N k^2} \sum_i (2J^{(i)}+1) P^{(i)}_{j_{12}^{ini} m_{12}'^{ini} j_1^{ini} j_2^{ini} \to j_1^{fin} j_2^{fin}} \quad (26)$$

which has to be substituted into eq 22. Note that sampling over J and l is done in one step (two-dimensional sampling), because there is no requirement that every term in eq 26 is converged. We only require that the entire sum in eq 26 is converged (i.e., only the average cross section, rather than each individual probability). Thus, the procedure is very efficient and only a moderate number of MQCT trajectories is needed.

III. NUMERICAL RESULTS

Theory developed in the previous section was applied to $N_2 + H_2$ system. We had no goal of describing this process as accurately as possible, or as completely as possible, but rather to test the equations we derived the computational methodology we developed and the codes we wrote so far. Thus, we only considered several exemplary state-to-state transition processes and have taken into consideration only a few terms in the potential energy expansion, just enough for these transitions to occur in the $N_2 + H_2$ collisions. The following terms of the potential energy expansion in eq 14 were included: A_{000}, A_{202}, A_{022}, and A_{224}. The potential energy surface of ref 40 was used.

In addition to MQCT calculations we also carried out the full-quantum CC-calculations using MOLSCAT[41] and used those as a benchmark. MOLSCAT calculations were much more demanding computationally, compared to MQCT calculations. In fact, for the results presented below, the range of collision energies and the size of rotational basis set were dictated by numerical cost of the full-quantum CC-calculations, not by MQCT. In some cases we intentionally have taken small basis set, to make the MOLSCAT calculations less costly. But, in all cases the MQCT and the MOLSCAT calculations were carried out with exactly the same rotational basis set and the same values of J^{max}, to make comparison straightforward and meaningful.

The first test case was rotational excitation of $N_2(j_1 = 0)$ by $H_2(j_2 = 2)$, with no rotational transitions allowed in H_2. Excitations of N_2 into $j_1 = 2$, 4, and 6 were analyzed. Thus, molecular basis set for H_2 included only one rotational state, $j_2 = 2$, whereas the basis set for N_2 included 9 rotational states, up to $j_1 = 16$. Only even values of j_1 were included, because homonuclear N_2 is symmetric, so that only transitions with even values of Δj are allowed (notice that these quantum properties can be rigorously described by MQCT). As explained in section II.4, our approach requires running $(2j_1^{ini}+1)(2j_2^{ini}+1)$ independent calculations. Accordingly, we carried out five calculations with initial states $-2 \le m_{12}' \le 2$ of $j_{12} = 2$. At low collision energies we used $J^{max} = 15$, whereas at high collision energies we used $J^{max} = 120$, in both full-quantum and MQCT calculations. Results are presented in Figure 1 for the range of collisional energies from the excitation threshold, which is 11.92 cm^{-1} for transition into $j_1 = 2$, up to the energy 4000 cm^{-1}.

The full-quantum benchmark data illustrate that energy dependencies of state-to-state cross sections are quite involved (Figure 2). For all three transitions the value of cross section rises

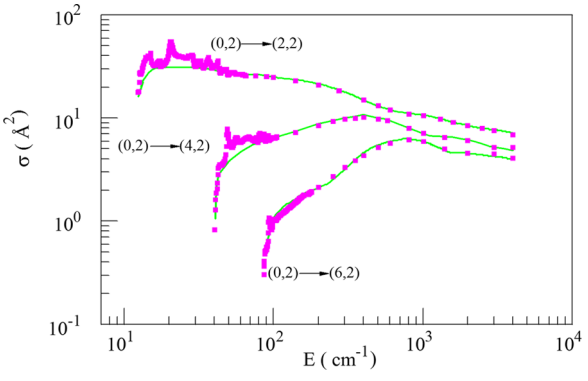

Figure 2. State-to-state cross sections for excitation of $N_2(j = 0)$ by collisions with $H_2(j = 2)$. Initial and final rotational states of collision partners are labeled as (j_1, j_2), where the first index belongs to N_2 whereas the second index belongs to H_2. Full-quantum benchmark data are shown by pink symbols, and results of MQCT are shown by green lines. See the text for a detailed description of this computational experiment.

DOI: 10.1021/acs.jpca.5b06812
J. Phys. Chem. A 2015, 119, 12329−12338

quickly at the corresponding threshold. Scattering resonances are observed in a short energy range just above the threshold, after which the dependence is smooth, but not necessarily monotonic. Thus, the dependencies for excitation of $j_1 = 4$ and 6 exhibit pronounced maxima near collision energies of 400 and 800 cm^{-1}, respectively. For excitation of $j_1 = 2$ the maximum is less important and is hidden by resonances at low energies, near 20 cm^{-1}. At higher energies cross sections for all three transitions tend to decrease. On top of these major trends, we also see some small-amplitude oscillations of cross section dependencies, most noticeable in the case of excitation into $j_1 = 2$ (Figure 2). Besides resonances, MQCT captures all these features. Even the excitation thresholds, and even the small oscillations of cross sections, are accurately reproduced.

At higher collision energies the results of MQCT become nearly identical to the full-quantum results (Figure 2). This, perhaps, is the most practically important aspect of MQCT, because the full-quantum calculations become prohibitively difficult at higher energies, whereas MQCT calculations remain affordable. At lower energies the treatment of resonances is probably possible within MQCT,[36] but this topic is beyond the scope of the present paper and is less important in practice, because the full-quantum calculations are quite affordable in the low-energy regime. Accurate description of the excitation thresholds within MQCT is possible due to the symmetrized approach,[22] also known as the average velocity approach, which we described in detail in our earlier paper.[28]

The second test case we chosen was a process of quenching of rotationally excited H_2 ($j_2 = 2$) into its ground state $j_2 = 0$ by collision with ground state N_2 ($j_1 = 0$). In these calculations the basis set included $j_1 = 0$ and 2 for N_2, and $j_2 = 0$ and 2 for H_2, which is just two states for each collision partner. Again, $(2j_1^{ini} + 1)(2j_2^{ini} + 1)$ of independent calculations were carried out, which is 5 for $j_{12} = 2$, with $-2 \le m'_{12} \le 2$. Note that this process does not have a threshold, because the internal rotational energy is released. The amount of energy released by H_2 is quite significant, close to 360 cm^{-1}, consistent with $\Delta j_2 = -2$. The range of collision energies considered here was also broad, from 1 up to 4000 cm^{-1}. MQCT results are presented in Figure 3, together with the full-quantum benchmark data obtained with MOLSCAT using the same basis set.

Figure 3 illustrates that, despite the fact that energy dependence of inelastic cross section is not simple for this state-to-state transition, the agreement between MQCT and the benchmark data is very good. Note that although there is no threshold for the process, the value of cross section changes by more than an order of magnitude through the range of considered energies and exhibits a pronounced minimum near collision energy of 60 cm^{-1}. In the low-energy regime the value of cross section growth resembles the asymptotic Wigner law.[42] Here MQCT is less accurate, which is expected from a method like MQCT (that incorporates a classical component) in the quantum scattering regime (where the asymptotic Wigner law behavior is typical). Several broad resonances in the energy range below 20 cm^{-1} (Figure 3) are reproduced by MQCT only on average. At higher energies the value of cross section also grows. Importantly, at collision energies above 50 cm^{-1} the results of MQCT are nearly identical to the full-quantum results.

To derive the scaling law of MQCT for the molecule + molecule case, we plotted in Figure 4 the computational cost of our calculations presented in Figure 2. The first frame, Figure 4a shows CPU time as a function of the number of channels. Here the notion of a "channel" should be discussed, because it is different from the channel in the molecule + atom case. Thus, in the molecule + atom case the channels are nondegenerate energy *levels*. Those are labeled by j in the case of the diatomic

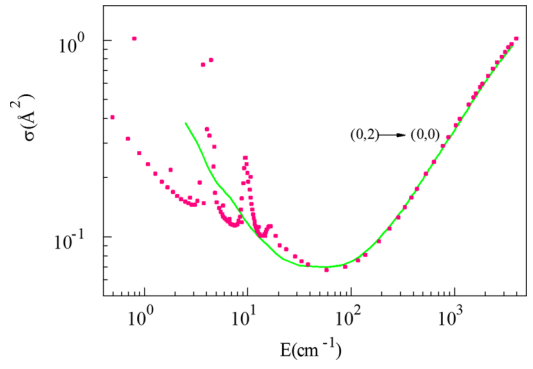

Figure 3. State-to-state cross sections for quenching of $H_2(j = 2)$ by collisions with $N_2(j = 0)$. Initial and final rotational states of collision partners are labeled as (j_1, j_2), where the first index belongs to N_2 whereas the second index belongs to H_2. Full-quantum benchmark data are shown by red symbols, and results of MQCT are shown by the green line. See the text for a detailed description of this computational experiment.

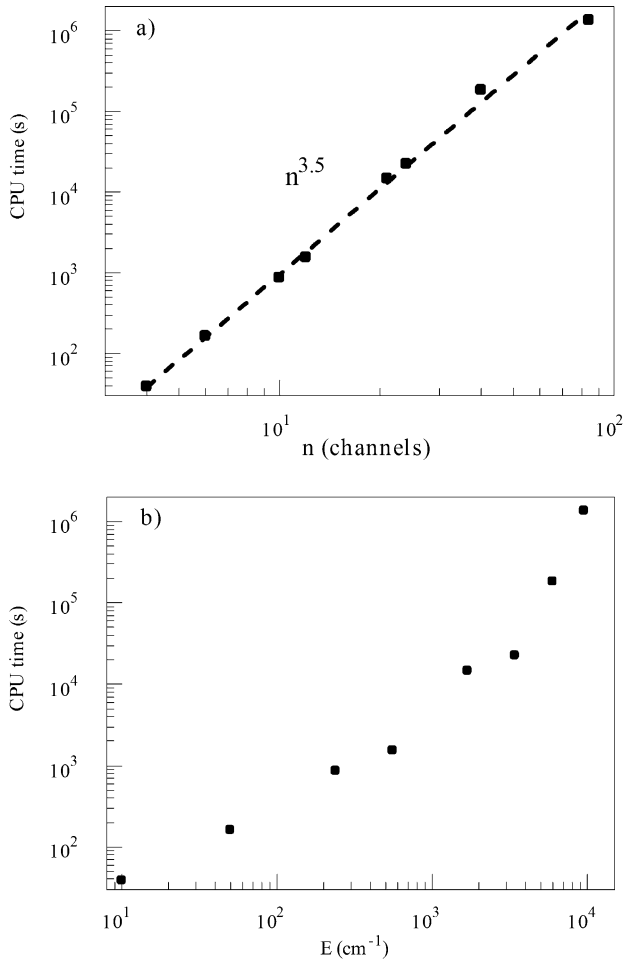

Figure 4. Computational cost of MQCT calculations presented in Figure 1 for $N_2 + H_2$. Two frames correspond to two different variables: (a) as a function of the number of channels included in calculations; (b) as a function of collision energy.

DOI: 10.1021/acs.jpca.5b06812
J. Phys. Chem. A 2015, 119, 12329−12338

molecule (or by $j_{k_a k_c}$ in the case of a general asymmetric top) and include $2j + 1$ degenerate *states* labeled by m', within each channel. In contrast, in the molecule + molecule case considered here the nondegenerate channels are labeled by the pairs of indexes (j_1, j_2). Such "channels" include $(2j_1 + 1)(2j_2 + 1)$ degenerate states labeled by j_{12}, and for each value of j_{12} they include the $2j_{12} + 1$ of degenerate projection states labeled by m'_{12}. So, the channels in the molecule + molecule case include more degenerate states than the channels in the molecule + atom case. Still, we prefer to analyze numerical performance as a function of channels, rather than a function of states, because this can be compared directly to the scaling law of the full-quantum calculations that also have channels but involve no projection states labeled by m'.

For example, in the previous work we found that the cost of fully converged MQCT for the molecule + atom case scales as $n^{2.5}$, where n is the number of channels. In this work we see from Figure 4a that the cost scales as $n^{3.5}$, which makes sense. The additional factor of n comes from the presence of additional degenerate states labeled by j_{12}. Note that this scaling law represents the overall cost of MQCT calculations, converged with respect to J^{max} at each collision energy. In contrast, when the scaling law of the full quantum calculations is discussed, it is usually reported for an idealized test, when the number of channels is changed, but the value of J^{max} and the number of partial scattering waves needed for convergence are kept constant. But in practice, when the collision energy is raised, the value of J^{max} needed for convergence also grows, and the cost of calculations increases dramatically, particularly for heavy collision partners. Although the scaling law of the full-quantum calculations with respect to the number of channels is only on the order of n^4 in an idealized situation, in reality, when the calculations are carried out for a broad energy range, the overall cost reaches n^6 to n^7. Importantly, in MQCT such "overhead" does not occur (because the scattering process is treated classically) and the cost remains low, $n^{3.5}$, as shown in Figure 4a.

In this respect we want to mention that the data presented in Figure 2 were reported only for collision energies below 4000 cm^{-1} due to significant computational cost of the MOLSCAT calculations at higher energies. Practical full-quantum calculations at higher collision energies would require the parallel version of MOLSCAT, which we did not use. However, MQCT calculations were quite efficient at even higher energies. For example, in Figure 4b we presented the cost of MQCT calculations as a function of collision energy up to 10000 cm^{-1}.

IV. CONCLUSIONS

We worked out the mixed quantum classical theory, MQCT, for inelastic collision of two molecules, where the internal (rotational) motion of the molecules is treated with quantum mechanics, whereas the molecule−molecule scattering is described by classical trajectories. The resultant MQCT formalism includes a system of coupled equations for quantum probability amplitudes, and the mean-field classical equations of motion. The procedure for sampling the initial conditions and computing cross sections has also been devised. Derivations presented here were carried out for two diatomic molecules treated as rigid rotors, but extension onto two polyatomic molecules, and inclusion of the vibrational states into the basis set, are both relatively straightforward. To our best knowledge such theory has never been formulated in the past.

We also carried out some numerical tests of this theory, using a real system $N_2 + H_2$ with accurate potential energy surface, for a broad range of collision energies and several most important state-to-state transitions. Besides scattering resonances at low collision energies (which we did not try to describe here) the full-quantum results were reproduced by MQCT in detail, including the excitation thresholds, the maxima of cross sections, some small oscillations of energy dependencies, and the asymptotic behavior. Most importantly, at higher energies the results of MQCT become nearly identical to the full quantum results. It looks like in this energy range MQCT is a good alternative to the full-quantum calculations, because the latter become computationally expensive. The scaling law (computational cost vs system complexity) was also determined for MQCT and was found to be much more favorable compared to that of the full-quantum calculations.

One way of using MQCT is by blending its results with results of the full-quantum CC calculations. Namely, to compute rate coefficients the values of cross sections are typically needed in a broad range of collision energies. One could start by running CC calculations at lower energies, because they are quite affordable there, and because scattering resonances may occur in this regime. At higher energies, where CC calculations become too demanding, one may start MQCT and check if it is in good agreement with CC method. If yes, one could stop CC calculations and continue with MQCT only, because it is more affordable and is sufficiently accurate at higher energies. The standard practice nowadays is to switch, at higher energies, from the exact CC to an approximate CS method. However, we showed in our recent work on several systems and in different collision regimes[33,35] that the fully coupled MQCT is more accurate than CS approximation, where centrifugal coupling is neglected and transitions between different m-states do not occur. So, switching to MQCT, instead of CS, may be more advantageous.

Several topics related to MQCT still require further work. Although less important from practical perspective, the question of scattering resonances is important from theoretical point of view. Earlier work by others indicates that it might be possible to use phase information to describe resonances within MQCT framework. Another question is collision of identical particles, such as $N_2 + N_2$, or $H_2 + H_2$. Present theory is only valid for nonidentical molecules. In the case of two identical molecules the total wave function should be properly symmetrized, and this seems to be feasible for MQCT. Also, it is an interesting question whether MQCT is capable of describing accurately the so-called quasi-resonant energy transfer between two molecules. We plan exploring some of these issues in the near future.

Finally, from the method development perspective, it would be interesting to formulate MQCT using grid representation (DVR) of the rotational wave function, instead of the basis set expansion (FBR) used here. Such treatment of rotational wave packets may be more efficient for molecules and processes where large number of rotational states is excited, leading to large state-to-state transition matrices that are difficult to handle. One important applications of such methodology would be in inelastic scattering by polyatomic molecules, where the spectra of rotational states are very dense.

AUTHOR INFORMATION

Corresponding Author

*D. Babikov. Electronic mail: dmitri.babikov@mu.edu.

DOI: 10.1021/acs.jpca.5b06812
J. Phys. Chem. A 2015, 119, 12329−12338

Notes

The authors declare no competing financial interest.

■ ACKNOWLEDGMENTS

This research was partially supported by NSF, through the grant AGS-1252486. This research used resources of the National Energy Research Scientific Computing Center, which is supported by the Office of Science of the U.S. Department of Energy under Contract No. DE-AC02-5CH11231.

■ REFERENCES

(1) Kirste, M.; Wang, X.; Schewe, H. C.; Meijer, G.; Liu, K.; van der Avoird, A.; Janssen, L. M.; Gubbels, K. B.; Groenenboom, G. C.; van de Meerakker, S. Y. Quantum-state resolved bimolecular collisions of velocity-controlled OH with NO radicals. *Science* **2012**, *338*, 1060−1063.

(2) Dagdigian, P.; Alexander, M. H. Theoretical investigation of rotationally inelastic collisions of the methyl radical with helium. *J. Chem. Phys.* **2011**, *135* (9), 064306−064306.

(3) Balakrishnan, N.; Groenenboom, G. C.; Krems, R. V.; Dalgarno, A. The He−CaH($^2\Sigma^+$) interaction. II. Collisions at cold and ultracold temperatures. *J. Chem. Phys.* **2003**, *118*, 7386−7393.

(4) Roueff, E.; Lique, F. Molecular excitation in the interstellar medium: Recent advances in collisional, radiative, and chemical processes. *Chem. Rev.* **2013**, *113*, 8906−8938.

(5) Daniel, F.; Dubernet, M.-L.; Grosjean, A. Rotational excitation of 45 levels of ortho/para-H_2O by excited ortho/para-H_2 from 5 to 1500 K: state-to-state, effective, and thermalized rate coefficients. *Astron. Astrophys.* **2011**, *536*, A76.

(6) dos Santos, F. S.; Balakrishnan, N.; Forrey, R. C.; Stancil, P. C. Vibration-vibration and vibration-translation energy transfer in H_2-H_2 collisions: A critical test of experiment with full-dimensional quantum dynamics. *J. Chem. Phys.* **2013**, *138* (10), 104302−104302.

(7) Song, H.; Lu, Y.; Lee, S.-Y. Fully converged integral cross sections of collision induced dissociation, four-center, and single exchange reactions, and accuracy of the centrifugal sudden approximation, in H_2 + D_2 reaction. *J. Chem. Phys.* **2012**, *136* (9), 114307−114307.

(8) Arthurs, A. M.; Dalgarno, A. The theory of scattering by a rigid rotator. *Proc. R. Soc. London, Ser. A* **1960**, *A256*, 540−551.

(9) Loreau, J.; Zhang, P.; Dalgarno, A. Elastic scattering and rotational excitation of nitrogen molecules by ssodium atoms. *J. Chem. Phys.* **2011**, *135* (8), 174301−174301.

(10) Yang, B.; Nagao, M.; Satomi, W.; Kimura, M.; Stancil, P. C. Rotational quenching of rotationally excited H2O in collisions with He. *Astrophys. J.* **2013**, *765* (9), 77−77.

(11) Schewe, H. C.; Ma, Q.; Vanhaecke, N.; Wang, X.; Kłos, J.; Alexander, M. H.; van de Meerakker, S. Y. T.; Meijer, G.; van der Avoird, A.; Dagdigian, P. J. Rotationally inelastic scattering of OH by molecular hydrogen: Theory and experiment. *J. Chem. Phys.* **2015**, *142* (13), 204310−204310.

(12) Faure, A.; Wiesenfeld, L.; Scribano, Y.; Ceccarelli, C. Rotational excitation of mono- and doubly-deuterated water by hydrogen molecules. *Mon. Not. R. Astron. Soc.* **2012**, *420*, 699−704.

(13) Mack, A.; Clark, T. K.; Forrey, R. C.; Balakrishnan, N.; Lee, T.-G.; Stancil, P. C. Cold He+H_2 collisions near dissociation. *Phys. Rev. A: At., Mol., Opt. Phys.* **2006**, *74* (8), 052718.

(14) Conte, R.; Houston, P. L.; Bowman, J. M. Trajectory study of energy transfer and unimolecular dissociation of highly excited allyl with argon. *J. Phys. Chem. A* **2014**, *118*, 7742−7757.

(15) Czakó, G.; Kaledin, A. L.; Bowman, J. M. A practical method to avoid zero-point leak in molecular dynamics calculations: Application to the water dimer. *J. Chem. Phys.* **2010**, *132* (6), 164103−164103.

(16) Babikov, D.; Walker, R. B.; Pack, R. T. A quantum symmetry preserving semiclassical method. *J. Chem. Phys.* **2002**, *117*, 8613−8622.

(17) Wang, Y.; Bowman, J. M. Mode-specific tunneling using the Q_{im} path: Theory and an application to full-dimensional malonaldehyde. *J. Chem. Phys.* **2013**, *139* (5), 154303−154303.

(18) Schinke, R.; Fleurat-Lessard, P. The effect of zero-point energy differences on the isotope dependence of the formation of ozone: A classical trajectory study. *J. Chem. Phys.* **2005**, *122* (9), 094317−094317.

(19) McCann, K. J.; Flannery, M. R. A multistate semiclassical orbital treatment of heavy-particle collisions with application to H+H_2 rotational transitions. *Chem. Phys. Lett.* **1975**, *35*, 124−130.

(20) McCann, K. J.; Flannery, M. R. New semiclassical treatments of rotational and vibrational transitions in heavy-particle collisions. I. H−H_2 and He−H_2 collisions. *J. Chem. Phys.* **1975**, *63*, 4695−4707.

(21) Billing, G. D. The semiclassical treatment of molecular roto-vibrational energy transfer. *Comput. Phys. Rep.* **1984**, *1*, 239−296.

(22) Billing, G. D. *The Quantum-Classical Theory*; Oxford University Press: Oxford, U.K., 2002.

(23) Avery, J.; Herman, Z. Gert Due Billing (1946−2002). *Chem. Soc. Rev.* **2003**, *32* (1), iv.

(24) Ivanov, M. V.; Babikov, D. Mixed quantum-classical theory for the collisional energy transfer and the ro-vibrational energy flow: Application to ozone stabilization. *J. Chem. Phys.* **2011**, *134* (16), 144107−144107.

(25) Ivanov, M. V.; Babikov, D. Efficient quantum-classical method for computing thermal rate constant of recombination: Application to ozone formation. *J. Chem. Phys.* **2012**, *136* (16), 184304−184304.

(26) Ivanov, M. V.; Babikov, D. On molecular origin of mass-independent fractionation of oxygen isotopes in the ozone forming recombination reaction. *Proc. Natl. Acad. Sci. U. S. A.* **2013**, *110* (5), 17708−17708.

(27) Semenov, A.; Babikov, D. Equivalence of the Ehrenfest theorem and the fluid-rotor model for mixed quantum/classical theory of collisional energy transfer. *J. Chem. Phys.* **2013**, *138* (10), 164110−164110.

(28) Semenov, A.; Ivanov, M. V.; Babikov, D. Ro-vibrational quenching of CO (v = 1) by He impact in a broad range of temperatures: A benchmark study using mixed quantum/classical inelastic scattering theory. *J. Chem. Phys.* **2013**, *139* (12), 074306−074306.

(29) Semenov, A.; Babikov, D. Mixed quantum/classical theory of rotationally and vibrationally inelastic scattering in space-fixed and body-fixed reference frames. *J. Chem. Phys.* **2013**, *139* (15), 174108−174108.

(30) Billing, G. D. Comparison of quantum mechanical and semiclassical cross sections for rotational excitation of hydrogen. *Chem. Phys. Lett.* **1977**, *50*, 320−323.

(31) Ivanov, M. V.; Dubernet, M.-L.; Babikov, D. Rotational quenching of H_2O by He: Mixed quantum/classical theory and comparison with quantum results. *J. Chem. Phys.* **2014**, *140* (7), 134301−134301.

(32) Semenov, A.; Babikov, D. Accurate calculations of rotationally inelastic scattering cross sections using mixed quantum/classical theory. *J. Phys. Chem. Lett.* **2014**, *5*, 275−278.

(33) Semenov, A.; Babikov, D. Mixed quantum/classical calculations of total and differential elastic and rotationally inelastic scattering cross sections for light and heavy reduced masses in a broad range of collision energies. *J. Chem. Phys.* **2014**, *140* (13), 044306−044306.

(34) Semenov, A.; Dubernet, M.-L.; Babikov, D. Mixed quantum/classical theory for inelastic scattering of asymmetric-top-rotor + atom in the body-fixed reference frame and application to the H_2O + He system. *J. Chem. Phys.* **2014**, *141* (8), 114304−114304.

(35) Semenov, A.; Babikov, D. Mixed quantum/classical approach for description of molecular collisions in astrophysical environments. *J. Phys. Chem. Lett.* **2015**, *6*, 1854−1858.

(36) McCann, K. J.; Flannery, M. R. Elastic scattering and rotational excitation in ion−molecule collisions. II. Li^+−H_2 and H^+−H_2 collisions. *J. Chem. Phys.* **1978**, *69*, 5275−5287.

(37) Green, S. Rotational excitation in H_2−H_2 collisions: Close-coupling calculations. *J. Chem. Phys.* **1975**, *62*, 2271−2282.

(38) Varshalovich, D. A.; Moskalev, A. N.; Khersonskii, V. K. *Quantum theory of angular momentum*; World Scientific: Singapore, 1988.

(39) Green, S. Rotational excitation of symmetric top molecules by collisions with atoms: Close coupling, coupled states, and effective potential calculations for NH_3−He. *J. Chem. Phys.* **1976**, *64*, 3463−3473.

DOI: 10.1021/acs.jpca.5b06812
J. Phys. Chem. A 2015, 119, 12329−12338

(40) Gomez, L.; Bussery-Honvault, B.; Cauchy, T.; Bartolomei, M.; Cappelletti, D.; Pirani, F. Global fits of new intermolecular ground state potential energy surfaces for N_2-H_2 and N_2-N_2 van der Waals dimers. *Chem. Phys. Lett.* **2007**, *445*, 99−107.
(41) Hutson, J. M.; Green, S. *MOLSCAT Computer Code*, version 14; 1994. Distributed by collaborative computational project No. 6 of the Engineering and Physical Sciences Research Council, Swindon, U.K.
(42) Balakrishnan, N.; Dalgarno, A.; Forrey, R. C. Vibrational relaxation of CO by ^{4}He at ultralow temperatures. *J. Chem. Phys.* **2000**, *113*, 621−632.

DOI: 10.1021/acs.jpca.5b06812
J. Phys. Chem. A 2015, 119, 12329−12338